Evidence of Parametric Decay Instability in Wendelstein 7-X stellarator

A.Tancetti[1], S.K. Nielsen[1], J. Rasmussen[1], D. Moseev[2], E.Z. Gusakov[3], A.Yu. Popov[3], T. Stange[2], S. Marsen[2], M. Zanini[2], C. Killer[2], M. Vecsei[4], H.P. Laqua[2] and W7-X Team

[1] *Department of Physics, Technical University of Denmark, Kgs. Lyngby, Denmark*

[2] *Max-Planck-Institut für Plasmaphysik, Greifswald, Germany*

[3] *Ioffe Institute, Saint-Petersburg, Russia*

[4]*Wigner Research Center for Physics, Budapest, Hungary*

Introduction: When a pump wave propagates in a plasma, it may decay into a pair of daughter waves, if the pump power exceeds a given threshold. This nonlinear interaction is known as Parametric Decay Instability (PDI) and has been observed in ionospheric [1] and in fusion plasmas [2]. In inhomogeneous plasmas, a substantial decrease of the power threshold occurs when daughter waves are trapped within a non-monotonic density profile [3]. In Wendelstein 7-X (W7-X) stellarator, high-power microwave beams, used for plasma heating and current drive, may decay within the density bump in a stationary magnetic island at the plasma edge. In this scenario, PDIs can reduce the efficiency of the heating system and hamper the optimal operation of microwave diagnostics. In the following, we present an overview of the theoretical model for PDI in W7-X and compare it with experimental evidence of PDI-related signals from campaign OP1.2.

Theoretical model: Figures 1(a) and (b) show the 1D density bump expected in the stationary magnetic island of W7-X and the cascade of nonlinear processes proposed in this scenario, respectively. In the primary stage, the pump beam, at frequency f_0, decays into a back-scattered X-mode wave, f_2, and a trapped upper hybrid wave (UHW), with frequency f_1 slightly smaller than $f_0/2$. Build-up of UHWs in the cavity is saturated by a secondary decay with excitation of slightly down-shifted UHWs, f_3, and low-frequency ion Bernstein waves (IBW), f_4, confined in the density bump. Since multiple nearby branches of the IB dispersion relation can be localized in the cavity, a number of harmonics, centered at f_4 and shifted by an ion cyclotron frequency, $f_{IC}^{edge} \approx 34$ MHz in the edge of W7-X, can be excited. Dispersion curves for the primary and secondary trapped UHWs are plotted in Figure 1(a). Here, we assume an hydrogen plasma with $T_e = 40\ eV$, provided by probes on the multi-purpose manipulator [4], and $B = 2.23$ T. Closed loops in the dispersion curves suggest confinement of the modes around the density local maximum. As shown by a comparison of the cyan dispersion curves, k^*, in Figures 1(a) and (c),

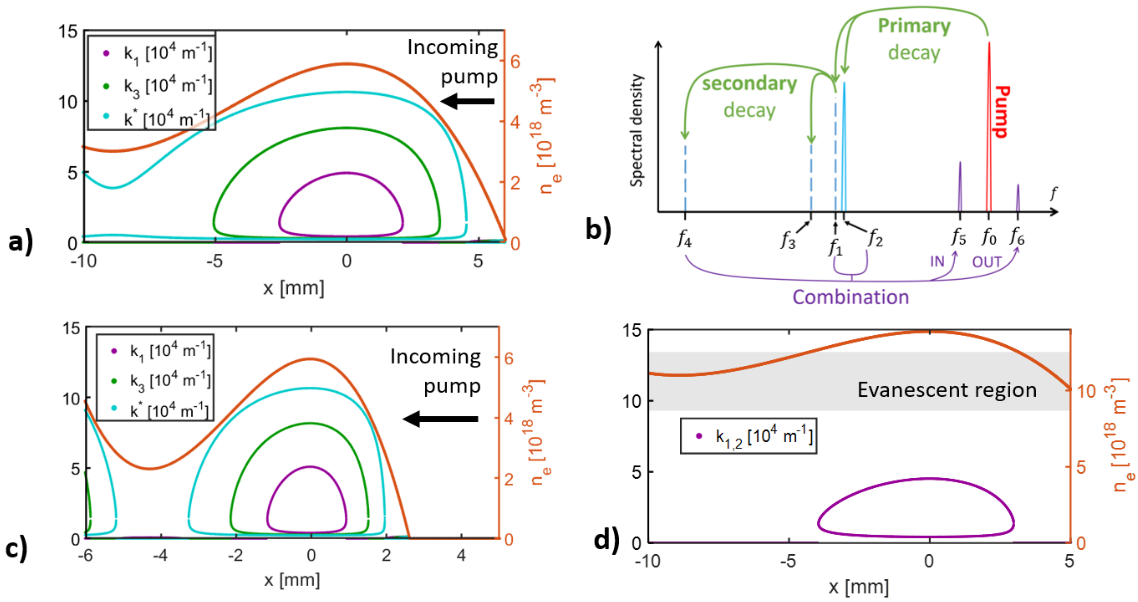

Figure 1. a) Predicted density bump in the magnetic island of W7-X, with maximum at x = 0 mm, and dispersion curves for primary (purple) and secondary (green) UHWs. b) PDI cascade in the density bump. c) Density profile and dispersion curves for the case of a tertiary decay, with additional confinement of an UHW with wave-vector k^* (cyan).and d) for the case of TPD.

additional modes are confined in a more prominent density bump, increasing the probability of a tertiary decay. In cascades with an even number of secondary decays, pump depletion seems to be the main mechanism of saturation for the primary instability and higher levels of pump power absorption are predicted [3]. Conversely, if the density bump lies within the evanescent region for the daughter X-mode, the decay is expected to be inhibited. It is worth noting, however, that if the bump emerges from the evanescent region (see Figure 1(d)), excitation of the two-plasmon decay (TPD) instability, where two trapped UHWs, at $f_{1,2} = f_0/2$, can take place.

Finally, the last step of the proposed PDI cascade implies the nonlinear combination of primary daughters with inward and outward propagating IBWs and generation of high-frequency electromagnetic modes directed toward the plasma edge, f_5, and f_6, respectively.

Measurements of PDI in W7-X: A Poincare plot of the standard magnetic configuration in W7-X is shown in Figure 2(a). Microwave beams, A1 and B1, are injected from mirrors on the right and cross the equatorial plane magnetic island before reaching the electron cyclotron resonance (ECR), in cyan. The magenta rays show the line of sight of the Collective Thomson Scattering (CTS) receiver [5].

High resolution edge density profiles are measured by alkali beam emission spectroscopy (ABES) [6] and plotted in Figure 2(b). The solid profile results from averaging over the start-up phase of the discharge, from $t = 0$ to 1 s, and highlights the possibility of a parametric cascade (compare with Figure 1(a)); conversely, the dashed curve, acquired immediately after $t =$ 1 s, falls into the evanescent region. Measurements of PDI-related structures with the CTS radiometer are presented in Figure 3(a). Lines in the central area are produced by the operative microwave beams, whereas PDI-related signals consist of a couple of sidebands stretching from $t = 0.2$ to 1 s, symmetrically arranged around the source A1. The frequency shift of the bands grows from $|\Delta f| = 0.75$ to 1 GHz. At $t = 1$ s, the PDI-related signal vanishes suggesting inhibition of the instability when propagation of the electromagnetic daughter is forbidden (see Figure 2(b)).

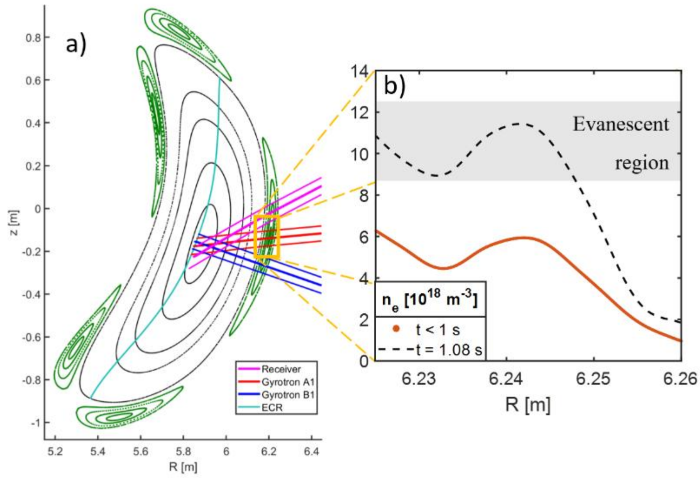

Figure 2. a) Poincare plot with green stationary magnetic islands, microwave (red, A1; blue, B1) and receiver (magenta) beams. b) ABES density profiles within the island for shot 20180821.12.

Clear peaks appear in the fine structure of each sideband and are plotted in Figure 3(b). Here, adjacent peaks are approximately 30 MHz away, suggesting excitation of IBWs in the edge. PDI in the edge is also indicated by correlation between the sidebands' intensity and events in the edge referred to as island localized modes (ILMs) [7]. Figure 4 offers a comparison between time-traces

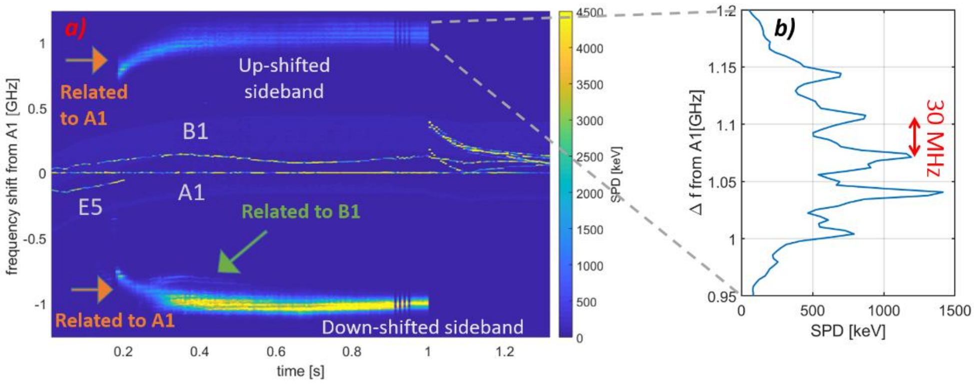

Figure 3. a) CTS mean spectrogram for experimental program 20180821.12 with frequency shift from A1 in the y-axis. b) Spectral power density (SPD) in the frequency interval of the up-shifted PDI-related band.

of the normalized PDI band intensity, edge temperature from channel 1 of the electron cyclotron emission spectroscopy, and the divertor Langmuir density in experimental program 20180821.17. Shaded areas highlight ILM-like events, occurring with a frequency close to 130 Hz. Peaks in the density profile measured on the divertor plate may be related to flattening of the island density profile with consequent suppression of the daughter trapping mechanism.

To assess the non-linear power scaling, a power ramp from $P_{A1} = 650$ to 150 kW was performed with plasma parameters different than those listed above. Here, the magnetic configuration is inward shifted, with a slightly higher magnetic field strength in the edge, and 50/50% gas composition of H/He. A power threshold was identified at $P_{XP} \approx 250$ kW, above which the sideband intensities grow exponentially with increasing pump power.

Summary: PDI-related signal was detected in operation OP1.2 in W7-X. Theoretical predictions can reproduce the power and the spectrum of the measured signal. Strong correlation of crashes in PDI sidebands with ILM-like events supports excitation of PDI in the plasma edge.

Acknowledgements: *This work has been supported by research grant 15483 from VILLUM FONDEN and the Enabling Research grant ENR-MFE19.DTU-03 from the EUROfusion Consortium. This work has been carried out within the framework of the EUROfusion Consortium and has received funding from the Euratom research and training programme 2014-2018 and 2019-2020 under grant agreement No 633053. The views and opinions expressed herein do not reflect those of the European Commission. The theoretical analysis was supported by the state contract of the Ioffe Institute.*

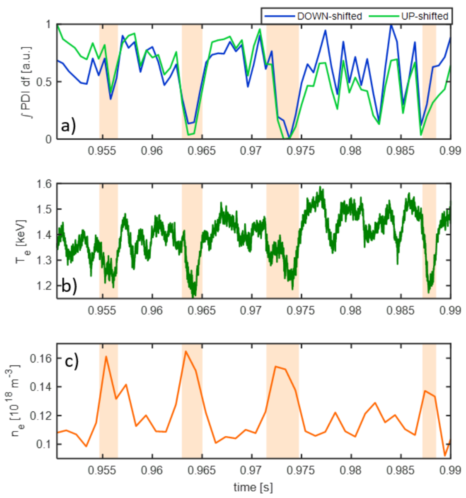

Figure 4. Simultaneous ILM-like events in PDI sidebands (a), edge electron temperature (b), and divertor density (c).

References

[1] A.V. Gurevich, *Physics – Uspekhi,* **50** (11) 1091-1121 (2007)

[2] R. Wilhelm *et al.*, *PPCF*, **26**, 1433 (1984)

[3] E.Z. Gusakov, and A.Yu. Popov, *Phys.Plasmas* **23**, 082503, (2016)

[4] C. Killer *et al*, *Nucl. Fusion* **59** 086013 (2019)

[5] D. Moseev *et al.*, *Rev. Sci. Instrum.* 90, 013503 (2019)

[6] M. Vécsei *et al.*, *45th EPS Conference on Plasma Physics*, ECA Vol.42A (2018)

[7] G.A. Wurden, *et al.*, *46th EPS Conference on Plasma Physics*, ECA Vol.43C (2019)